Chemical Engineering Journal 117 (2006) 61–69

Chemical Engineering Journal

www.elsevier.com/locate/cej

Solvent-based cleaning of emulsion polymerization reactors

J.Y.M. Chew [a], S.J. Tonneijk [b], W.R. Paterson [a], D.I. Wilson [a,*]

[a] *Department of Chemical Engineering, New Museums Site, Pembroke Street, Cambridge CB2 3RA, United Kingdom*
[b] *NeoResins, Sluisweg 12, P.O. Box 123, 5140 AC Waalwijk, The Netherlands*

Received 7 June 2005; received in revised form 1 November 2005; accepted 9 November 2005

Abstract

Fluid dynamic gauging (FDG) has been used to study the kinetics of the cleaning, from various solid surfaces, of polymer layers representative of polymerization reactor foulants. Currently, solvents such as methylethylketone (MEK) are used for cleaning and it is desired to replace this with aqueous systems with less severe environmental impact. Laboratory-prepared samples of two polystyrene co-polymers and samples prepared in an industrial pilot plant were treated with two alkaline solutions, sodium hydroxide (NaOH) and sodium metasilicate, with an aqueous commercial cleaning agent (TPU) and with the organic solvent MEK. Single and composite layers were studied, and a variety of outcomes observed. The simple alkalis swelled the polymers but did not clean: MEK and TPU swelled and then cleaned off both laboratory films, the mechanism varying between cohesive breakdown and adhesive detachment for different polymer/solvent combinations. One pilot plant material behaved as its laboratory analogue, while another, which was not tested in the laboratory, left a residual film on the surface. Experiments on composite layers exhibited a rich diversity of behaviours which could be modelled as combinations of single film characteristics.

Keywords: Cleaning; Emulsion polymerization; Polymers; Swelling

1. Introduction

Fouling is a persistent operating problem in many polymerization reactor systems where fouling layers are generated by reactants and/or products sticking to the walls or internals (e.g. El-Aasser and Sudol [1]). These unwanted surface layers reduce heat transfer efficiency and can cause cross-contamination between batches, which is problematic when feedstocks are varied regularly. Fouling occurs in emulsion polymerization reactors via a number of mechanisms, which are described in detail by Vanderhoff [2]: major causes are loss of colloidal stability, where the emulsion forms a coagulum, and alternative polymerization pathways which form insoluble fouling precursors. Fouling can be reduced by careful control of composition and operating conditions but poor mixing in large reactors can result in local conditions which promote deposition. Reactor surfaces can be treated to reduce adhesion of films or inhibit reaction but this is not always feasible if feedstocks vary widely, aggressive cleaning is required or funding is limited. In large-scale production it may increase reactor down-time, thereby lengthening cycle times unpredictably, and reducing yields. The most cost-effective solution must therefore consider mitigation options for fouling, cleaning and waste minimization (e.g. Perka et al. [3]).

Regular cleaning is therefore necessary, and may employ chemical agents (e.g. soaking or spraying with solvents to soften and/or dissolve deposited material), hydraulic action (jets or sprays to shear material off) or a combination of both. The choice of chemical cleaning agent and operating methodology is often based on empirical testing. Similarly, predicting the effect of a physical treatment such as jetting requires detailed knowledge of the strength and rupture behaviour of a fouling layer. Obtaining reliable data for a physically based model of removal poses several challenges, although spinning disk techniques have been used with some success to quantify dissolution and mass transfer characteristics of polymer layers and mineral scales, e.g. Hunek and Cussler [4] and Kabin et al. [5,6]. For physical cleaning mechanisms, both the stress imposed by the flow and the mechanical strength of the foulant need to be quantified. The mechanical strength of fouling layers of thickness >100 μm can now be quantified using micro-mechanical devices (e.g. Liu et al. [7]), whereas technical studies of jet and spray ball cleaning

Abbreviations: FDG, fluid dynamic gauging; MEK, methylethylketone; NaOH, sodium hydroxide; PMMA, polymethylmethacrylate; PS, polystyrene; TPU, commercial cleaning agent

* Corresponding author.
E-mail address: ian_wilson@cheng.cam.ac.uk (D.I. Wilson).

1385-8947/$ – see front matter © 2005 Elsevier B.V. All rights reserved.
doi:10.1016/j.cej.2005.11.019

Nomenclature

d	tube diameter (m)
d_t	nozzle throat (m)
h	clearance (m)
m	gauging liquid mass flow rate (m)
s	suction head (m)
t	time (s)
T_g	Glass transition temperature (°C)
x	volume fraction of swollen polymer

Greek letters

δ	foulant layer thickness (m)
ε_{max}	maximum extent of swelling

Subscripts

max	maximum
o	initial

in the process sector are relatively sparse, although Morison and Thorpe [8] have reported the flow distribution in a spray-ball system which could be used to estimate shear stresses imposed on a fouling layer. Recent changes in environmental legislation mean that selection of cleaning technology now also needs to consider the environmental impact of the fluids used and their disposal. Organic solvents such as methylethylketone (MEK), although very effective, carry large environmental impact penalties and the use of alternative solvents, preferably aqueous ones, is receiving considerable attention.

This paper reports the use of the non-contact technique of fluid dynamic gauging, FDG, to monitor and thereby compare the cleaning characteristics of different solvents on a number of fouling layers generated by emulsion polymerization on laboratory test sections and in an industrial pilot plant. FDG was developed by Tuladhar et al. [9] as a method for tracking the dynamic swelling and removal of denatured whey protein deposits on stainless steels which swell markedly in alkali. Fig. 1 illustrates the concept: a convergent nozzle with throat diameter d_t is located near, but not in contact with, a semi-rigid and impermeable deposit surface immersed in an inviscid Newtonian liquid, at

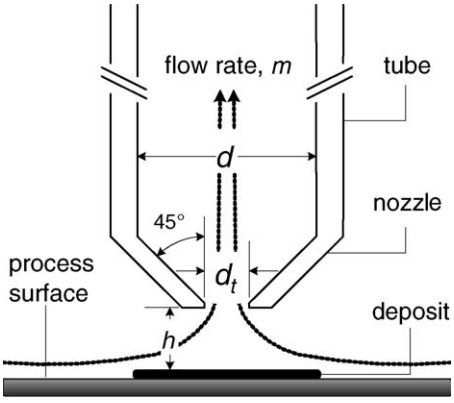

Fig. 1. Schematic of FDG operation.

Table 1
Polymer film properties

	PX/PPX	PA	PPM
Molecular mass (kDa)[a]	30	125	150
Acid content (wt%)[a]	7	5	2
Hansen solubility parameter ($MPa^{0.5}$)[a]	18.42	19.81	18.81
T_g[b] (Perkin-Elmer Pyris 1 DSC, 100 K/min)[b] (°C)	39	46	4

[a] Supplied by NeoResins.
[b] Analysis by D. Barker, Cambridge.

a clearance h. A steady suction pressure difference is applied so that liquid flows from the quasi-stagnant bulk into the nozzle; the flow rate of liquid is measured and yields h with good accuracy as long as $h/d_t < 0.25$. The accuracy of measurement depends on the geometry and instrumentation but for the $d_t = 1$ mm nozzle employed in this work the precision was ~10 μm. Knowledge of the nozzle location relative to the surface underneath the layer then yields the thickness of the deposit, δ.

Computational fluid dynamics (CFD) simulations of the flow regime under the nozzle lip [10] can then yield estimates of the stresses imposed on the surface, which can be linked to hydraulic conditions during cleaning. FDG was derived from pneumatic gauging, developed by Macleod and Todd [11] to monitor the thickness of solvent-swollen rubbers, which employed an emerging jet of air as the gauging fluid. Here, it is being used to monitor the swelling of synthetic polymers immersed in liquid solvents, via an effluent flow.

2. Experimental

Laboratory tests were performed on two types of proprietary polystyrene (PS) co-polymers, termed PX and PA. Table 1 summarises some characteristic properties of these materials. Pilot plant samples featured a second PS co-polymer, PPX, with properties identical to PX, and a polymethylmethacrylate (PMMA) co-polymer, labelled PPM. Laboratory test films were deposited on 50 mm diameter 316 stainless steel disks. Layers were generated from latex suspensions at room temperature using 0.20 and 0.08 mm wet film rollers. The applied film was left to settle for 4 h, then dried in a vacuum oven for 12 h at 50 °C. Films shrank to 50% of their initial thickness over the drying stage. Further coats could then be applied to the dried film to build up the initial film thickness or create composite films (here, up to 300 μm thick). Pilot plant samples were deposited on longer 316 stainless steel plates (width 25 mm, length 150 mm and thickness 1 mm) fixed to the walls or baffles of a semi-batch emulsion polymerization unit. These were removed, rinsed with reverse osmosis water and immersed in water containing a biocide before shipping to the laboratory for FDG testing.

Two FDG devices were used to monitor swelling and removal in this work. Both employed similar nozzle configurations and differed in the liquid bath arrangement. Fig. 2(a) shows the open system used for involatile and less aggressive solvents (here, aqueous NaOH and sodium metasilicate solutions), while Fig. 2(b) shows the contained system used for experiments with

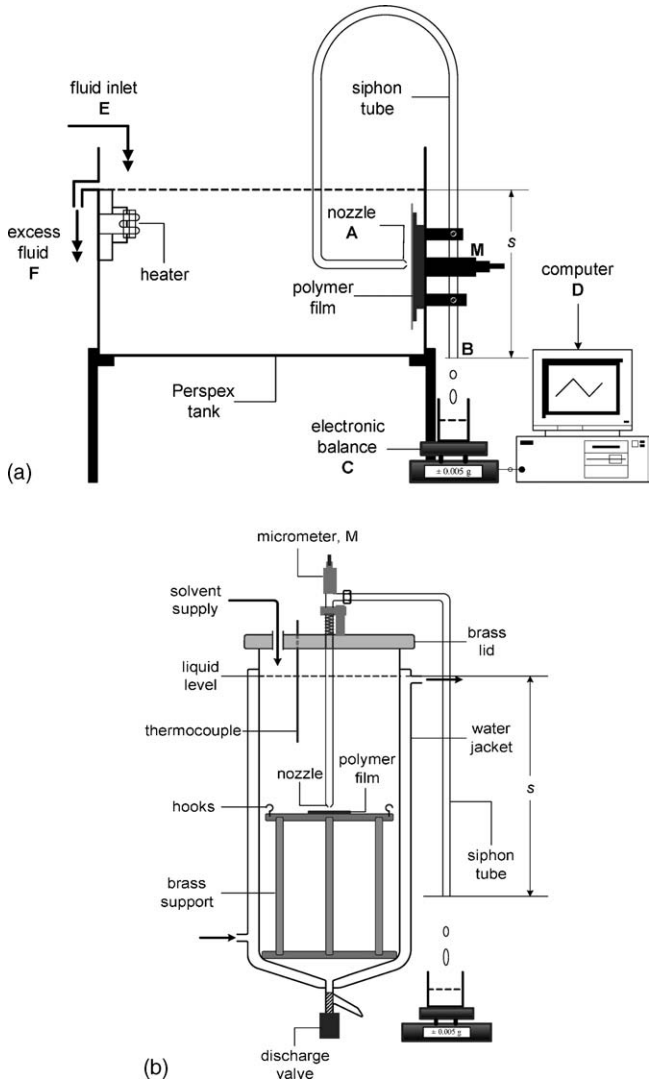

Fig. 2. FDG apparatus: (a) open system and (b) contained solvent system.

MEK and a commercial cleaning agent, TPU. Detailed descriptions of the apparatus are given in Chew [12].

The operating modes were identical. A flow or weir arrangement is used to maintain a constant liquid level while the suction driving head, s, is controlled by moving the open end of the siphon tube. The position of the gauging nozzle relative to the plate is controlled using the micrometer M, although the item manipulated by M differs between the units. The flow rate is measured using a gravimetric balance (±0.005 g) connected to a computer. Once the plate was fixed in position, thereby setting the start time, and a steady flow established, the clearance was adjusted to give a flow rate in the band corresponding to h values of 100–200 μm. This initial adjustment period usually lasted for around 2 min, so no data were available near time zero. At low h values, i.e. 40 μm or less, the gauging flow could cause visible deformation of the swollen polymer layer.

The potential for the gauging technique to influence film behaviour, either by surface shear or enhancement of mass transfer, was tested by performing pairs of experiments under identical process conditions. In the control experiment, the gauge was positioned near the surface (at 100 μm < h < 200 μm) throughout, while in the other the gauge was moved completely away from the surface (e.g. h > 15 mm) for periods of 1–2 min, then returned to the gauging length. For all conditions tested, the thickness–time profiles agreed within the accuracy of the technique and were comparable with duplicated experiments, indicating that the gauging technique did not influence film behaviour.

Four solvents were compared: aqueous solutions of sodium hydroxide (NaOH) and sodium metasilicate, methylethylketone (>99% 2-butanone) (all supplied by Fisher, Loughborough, UK) and Transol Production Unit (TPU, NL). TPU is a commercial blend of surfactants and dispersants based on an aqueous solution of sodium metasilicate with pH ∼ 12.8. Aqueous NaOH and metasilicate solutions were prepared by dissolving NaOH and sodium metasilicate pellets in reverse osmosis water. Fume hood limitations restricted MEK experiments to 60 °C, whereas the other solvents were studied up to 90 °C.

3. Results and discussion

3.1. Non-solvent action

Fig. 3 shows the thickness profiles observed for PA exposed to NaOH at different temperatures. Similar profiles were obtained with PX, and for both polymers swelling was not observed until temperatures exceeded 30 °C. After an initial induction period, which was longer for the larger molecular mass PA than with PX, the polymer swelled in a linear manner until it reached a plateau level, labelled δ_{max}. The induction period length decreased with increasing temperature in an Arrhenius fashion described by activation energies of 12 ± 1 kJ mol^{-1} (PA) and 25 ± 3 kJ mol^{-1} (PX). The maximum extent of swelling, ε_{max}, was defined as

$$\varepsilon_{max} = \frac{\delta_{max} - \delta_o}{\delta_o} \quad (1)$$

where δ_o was the thickness of the initial dry film. The swelling profiles of both polymers correspond to ε_{max} values > 1, i.e. beyond that of simple rehydration to the original wet film thickness. The films did not rehydrate or swell when exposed to water at pH 7. No reduction in film thickness over time was observed during the plateau phase, indicating that NaOH is a non-solvent.

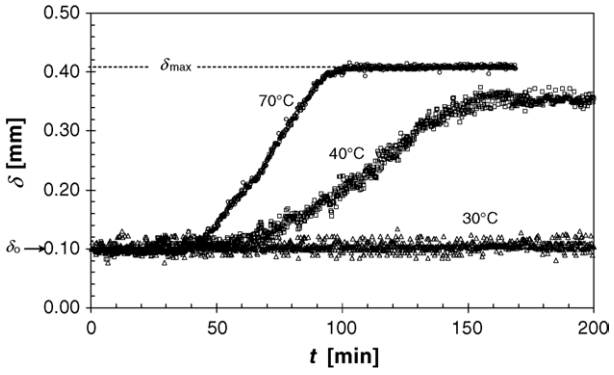

Fig. 3. Film thickness profiles for PA in NaOH. Laboratory films, δ_o = 100 μm.

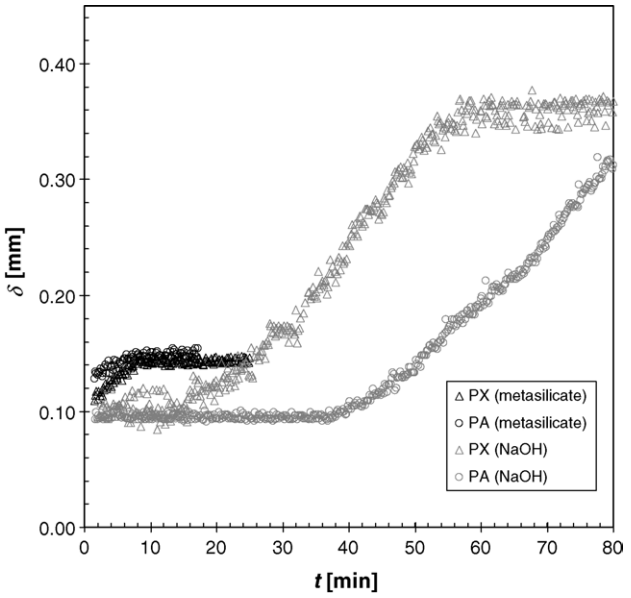

Fig. 4. Swelling profiles of PA (triangles) and PX (circles) in aqueous sodium metasilicate (black symbols, 90 °C) and sodium hydroxide (grey symbols, 70 °C) at pH 12.8 (corresponding to TPU). Laboratory films, δ_o = 100 μm.

This was confirmed by use of a second base, sodium metasilicate at 90 °C and pH 12.8 (that of the TPU solution), as shown in Fig. 4. No induction period is observed in the metasilicate for either polymer, while linear growth and a plateau phase, corresponding to different ε_{max} values, are again evident.

These results indicate that alkaline solutions are non-solvents for these polymer films, promoting swelling via charge interactions as the alkali neutralizes acid groups present in the polymer but without any dissolution of bonds between chains. The effect of temperature and hydroxide concentration on extent of swelling and rate varied with the nature of the polymer, and exhibited noticeable differences above and below the T_g value. Induction periods were longer for PA, which is consistent with its larger molecular mass, while the swelling rate for PX overtook that for PA at higher temperatures.

The linear swelling profiles indicate that swelling is not controlled by Fickian diffusion of hydroxide ion through the swollen layer: separate tests showed that the (linear) rate of swelling was independent of initial film thickness, indicating that swelling was controlled by a Case II diffusion mechanism [13]. The temperature dependency of swelling was characterized using a simple Arrhenius relationship and the Williams–Landel–Ferry (WLF) model [14] used for polymer melts and solutions. The data did not fit WLF kinetics but gave reasonable agreement with the Arrhenius model, yielding activation energies of 21 and 35 kJ mol^{-1} for PA and PX, respectively.

3.2. Solvent cleaning

Fig. 5 shows the behaviour of PX films in MEK at different temperatures. Swelling starts almost immediately, i.e. there is no induction period, and again exhibits an initial nearly linear profile followed by a short-lived plateau stage and a linear

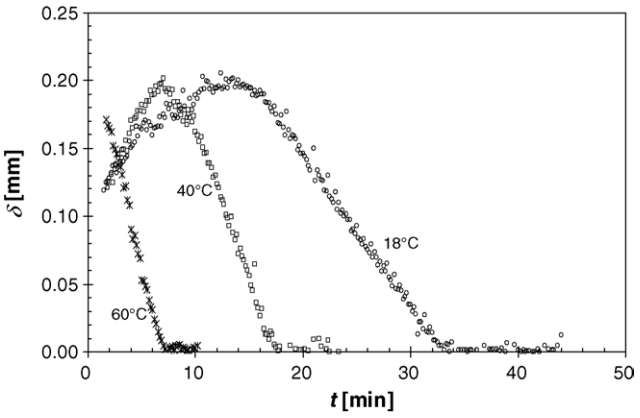

Fig. 5. PX film thickness profiles in MEK. Laboratory films, δ_o = 100 μm.

decay stage. Similar profiles were observed with PA, at different rates. The swelling rates were independent of initial film thickness, again indicating a Case II diffusion mechanism. The ε_{max} values were smaller than those observed in alkaline solvents, due to the removal process starting earlier, resulting in a short-lived plateau stage, if one exists at all. The removal rate was not affected by surface shear or mass transfer rates, indicating that the controlling processes are internal steps such as reptation (disentanglement of polymer chains), swelling and dissolution of polymer chains as reported by Devotta et al. [15]. Quantitative parameters describing the profiles, such as linear rates, ε_{max}, etc., were strongly affected by temperature. The activation energies of rate of swelling and rate of dissolution for both polymers again lay within the range 10–25 kJ mol^{-1}.

MEK is clearly an effective solvent for both polymers. MEK caused swelling and dissolution at 18 °C, whereas the films did not interact visibly with the alkaline solutions at 30 °C or lower. MEK is, however, a volatile and hazardous liquid and one of the aims of this work was to assess alternatives to its use in reactor cleaning.

TPU is a formulated alkaline solution and Fig. 6 shows that it is able to remove both PX and PA films, although by starkly different mechanisms. The PX profiles in Fig. 6(a) show similar behaviour to those observed for MEK, although at generally slower rates. No induction periods were observed and the extent of swelling was smaller than in MEK. The rate of swelling and ε_{max} were insensitive to initial film thickness, as before. Fig. 6(b) indicates a very different removal mechanism for PA films in TPU. The layers started to swell in a linear manner as soon as they were exposed to the solvent until they reached the point of complete swelling, when the film instantaneously detached itself from the solid surface. This detachment occurred in the absence of dynamic gauging, e.g. when immersing the deposited PA films in a beaker filled with TPU, and on a range of different surfaces, including glass, copper, stainless steel and other latex films, indicating that adhesive failure was the controlling mechanism. Cohesive breakdown occurs in the other cases, where the links between the polymer chains are broken in order that small units may dissolve. The cohesion within the PA films was still evident after detachment as the experimenter could manipulate and move the films through the liquid. These results suggest

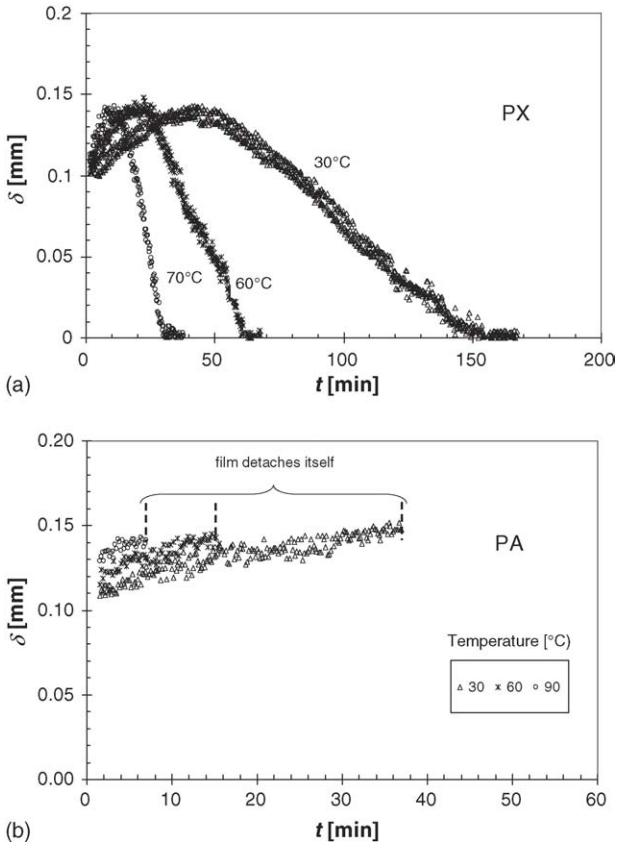

Fig. 6. Film thickness profiles in TPU: (a) PX including duplicated runs at 30 °C and (b) PA. Laboratory films, δ_o = 100 μm.

that the surfactants and other additives in TPU are breaking surface–polymer linkages in these layers.

Fig. 7(a) compares the swelling time and total time to clean PX, and it can be seen that TPU was slower than MEK across the whole temperature range studied; both solvents removed the whole fouling layer. Using TPU to clean PX films would therefore reduce the chemical hazard compared to MEK, at the cost of longer down-time for cleaning. Fig. 7(b) shows that TPU is as fast as MEK as long as the detached film can be removed, and there is therefore a good case for its use in cleaning reactors processing PA.

3.3. Composite layers

We now consider composite layers of foulant, mimicking the situation where extended cleaning is performed at the end of a series of reaction cycles. Experiments were performed on films composed of different layers on a stainless steel surface, e.g. [SS 316:100 μm PX:100 μm PA] and [SS 316:100 μm PA:100 μm PX]. Fig. 8 shows the removal profiles for composite films in TPU at 60 °C. The reader is reminded that the upper layer is deposited on the bottom layer after the latter has been dried. When PA was laid on top of PX, the PA layer swelled and detached, leaving the PX layer to dissolve off at a very similar rate to that observed for a PX layer in isolation. Most interestingly, when PX was laid on top of PA, the swelling profiles showed a change of slope consistent with the different rates of

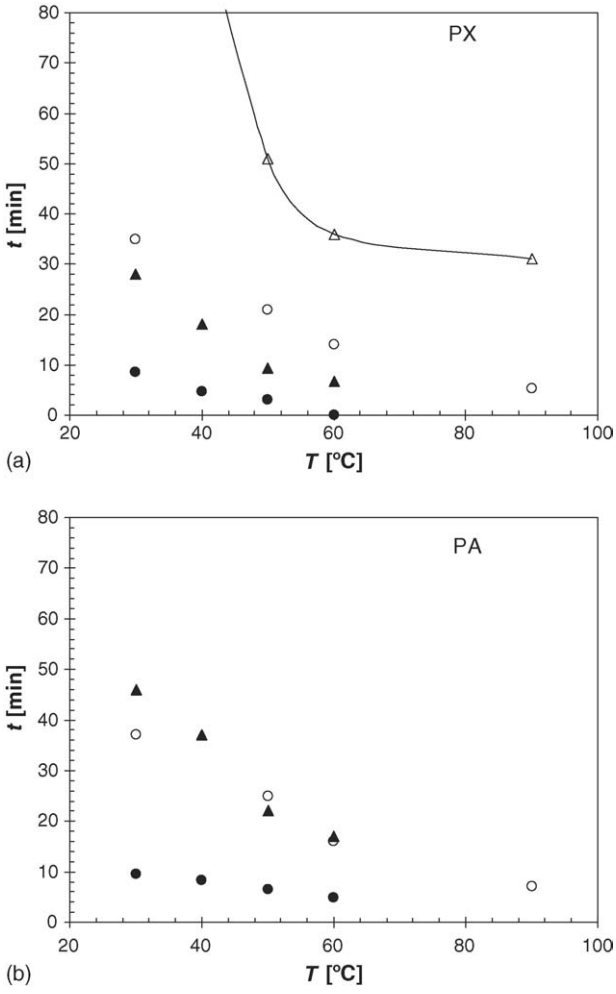

Fig. 7. Comparison of cleaning performance of solvents: (a) PX and (b) PA. (Circles) Time to swell and (triangles) time for complete cleaning. (Solid symbols) MEK and (open symbols) TPU. Laboratory films, δ_o = 100 μm.

swelling for the two polymers observed in single-component studies and detachment of a composite swollen film once the PA had reached the end of its swelling stage and adhesive failure occurred. In this case the PA film carried off the PX layer with it completely. These observations were evident at differ-

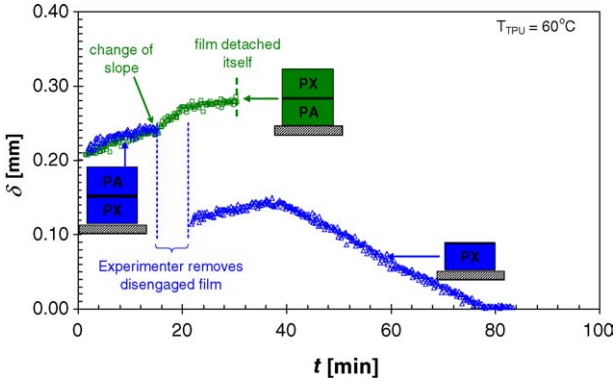

Fig. 8. Removal of simple composite films of PX and PA using TPU: (squares) PX on top of PA and (triangles) PA on PX. Laboratory films, δ_o = 200 μm, from 2 × 100 μm layers (after Chew et al. [18]).

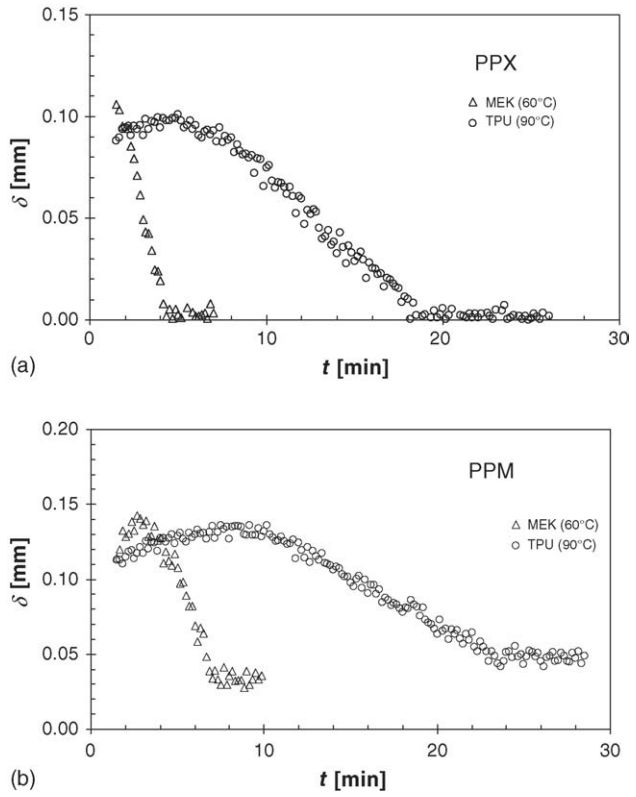

Fig. 9. Thickness profiles of pilot plant samples: (a) PPX and (b) PPM. (Triangles) MEK at 60 °C and (circles) TPU at 90 °C.

ent temperatures. Furthermore, calculations indicated that the time to remove all material could be predicted reliably from the experiments on layers of uniform composition.

This result indicates that scheduling of reactor batches can be exploited to enhance cleaning, and particularly to overcome the relatively slow performance of TPU as a solvent for PX compared to MEK. Rather than relying on the solvent to clean by breaking down cohesive interactions within the layer, the figure indicates that the adhesive failure mode with PA can be exploited to remove swollen material attached to this layer, in effect cleaving the fouling layer off the surface.

3.4. Pilot plant studies

The use of FDG to study individual and composite layer cleaning behaviours and thereby rank solvents and optimize operating protocols is now applied to compare laboratory tests with pilot plant material. Aged pilot plant samples of PPX and PPM were supplied by NeoResins. Fig. 9 shows the removal profiles of PPX and PPM, respectively, using MEK (at 60 °C) and TPU (at 90 °C). It should be noted that the initial film thicknesses differ even though the test plates were taken from the same reactor, confirming that fouling in the reactors is non-uniform.

Fig. 9(a) shows that the removal profiles for PPX in MEK and TPU are similar to those observed for PX (e.g. Figs. 5 and 6(a)): both solvents remove the layers completely. The rates of swelling, dissolution and ε_{max} are compared in Table 2. The rates of dissolution for PX and PPX in both solvents are close,

Table 2
Comparison of cleaning parameters extracted from cleaning profiles for PX (laboratory) and pilot plant layers

Solvent	Film		
	PX	PPX	PPM
MEK at 60 °C			
Rate of swelling [μm/min]	[a]	[a]	24
Rate of dissolution [μm/min]	34	35	27
ε_{max}	0.80	0.57	0.71
Residue depth [mm]	0	0	0.04
TPU at 90 °C			
Rate of swelling [μm/min]	7.2	6.3	6.2
Rate of dissolution [μm/min]	7.7	7.5	6.3
ε_{max}	0.39	0.25	0.42
Residue depth [mm]	–	–	0.05

[a] Swelling too rapid to measure.

agreeing to within 3%, indicating that the results obtained with laboratory samples are directly applicable to the pilot plant material. The rates of swelling and maximum extents of swelling differ appreciably. The ε_{max} values for the pilot plant samples are smaller, which is partly due to these parameters being calculated using the initial measured wet film thicknesses since they were supplied immersed in biocide solution; there were not many samples available, so drying these to determine the dry film thickness was not viewed as a priority. The initial wet film thicknesses were estimated by extrapolating the removal profiles to $t = 0$ min. Once more, TPU proved to act more slowly than MEK both at swelling and dissolving the films.

The removal profiles for PPM, plotted in Fig. 9(b), show the three characteristic stages mentioned previously but feature incomplete cleaning: a residual layer of thickness 40–50 μm remained on the steel plate. These residual layers could be readily scraped off with a fingernail or spatula, indicating that soaking and swelling weaken the adhesive bonds of the fouling layers (the original layer could not be scraped off easily). Extended soaking in either solvent did not remove the residual layer. Chemical analysis of the residual layer was not performed, partly due to the limited number of pilot plant samples. The layers are too thick to be adsorbed layers, which Hinsberg et al. [16] observed with some materials on quartz crystal microbalance surfaces. From a practical standpoint, this material is then suited to hydraulic removal using lances or spray-balls depending on the force required to disrupt the layer. FDG can be used to assess the strength of such layers (e.g. Chew et al. [17]) but there were not enough samples available in this case for such testing. The difference in cleaning behaviour between the PPX and PPM highlights the role of the polymer as well as the solvent. Avoiding the formation of the differently structured surface layer in PPM would be another strategy for enhancing cleaning.

The study of composite films in the laboratory was repeated in the pilot plant using PPM and PPX by generating films in successive batch reactions with different monomers. The reactor was rinsed out between batches. Fig. 10 shows the removal profiles obtained for these composites in TPU and the characteristic parameters are compared in Table 3. The fraction, and hence the initial thickness, of each polymer present in the composites

Table 3
Comparison of cleaning parameters extracted from cleaning profiles for pilot plant composite layers

	MEK at 60 °C		TPU at 90 °C	
	PPM/PPX[a]	PPX/PPM[a]	PPM/PPX[a]	PPX/PPM[a]
Rate of swelling [μm/min]	29	27	6.1	5.9
Dissolution rate [μm/min]	31	29	7.1	7.0
ε_{max}	0.65	0.64	0.32	0.33
Residue depth [mm]	0.12	0.05	0.13	0.04

Layer arrangements: top/bottom.
[a] Film.

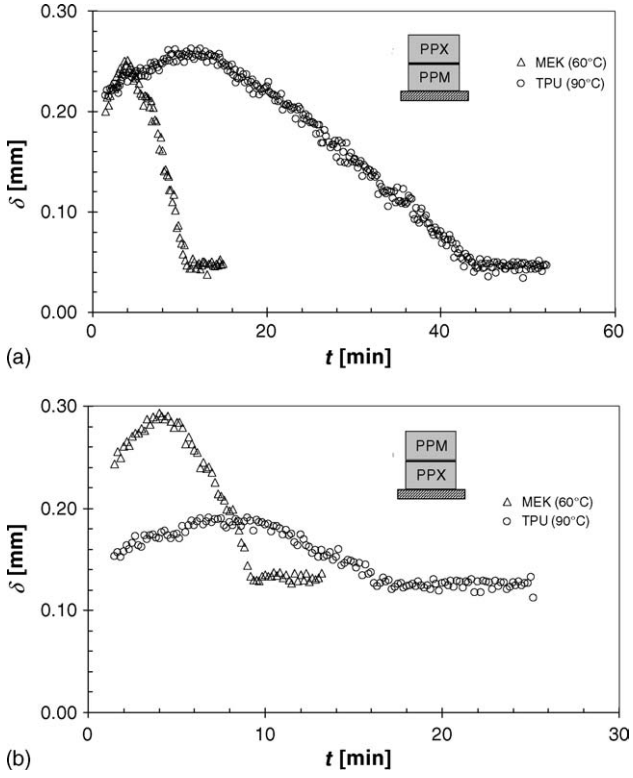

Fig. 10. Cleaning profiles of pilot plant composite films in MEK at 60 °C and in TPU at 90 °C: (a) PPX layer on top of PPM and (b) PPM layer on PPX.

is unknown. Also, the change in the swelling rate observed in Fig. 8 was not discernible here because the rates of swelling of PPX and PPM in TPU are similar, and swelling in MEK was rapid. Thus, the location of the interface of the two different layers was not obvious. More sophisticated techniques such as laser interferometry, as reported by Hinsberg et al. [16] for nanometer thick films, would be required to distinguish individual layers.

The thicknesses of the residual layers when the PPM layer was deposited directly on to the metal surface were similar to those in Fig. 9(b). It is reasonable to speculate that the residues consisted of PPM alone since PPX dissolved completely in TPU and MEK. This postulation was supported by a simple analysis on the TPU case outlined in Appendix A. Here, it was assumed that the bottom layer only started to swell to maximum thickness only after the top layer had swelled completely.

An important feature of the profiles in Fig. 10(b) is the depth of the residues obtained when PPX was the bottom layer; these were thicker than those remaining when PPM was the bottom layer or when PPM was the only material present. In this case, it is postulated that the residual layer in this case consists of a PPM residue layer and, beneath it, swollen PPX. The PPM residual layer formed a protective 'membrane' which allowed the solvent to penetrate and swell the PPX but did not permit swollen PPX to dissolve away. The simple analysis outlined in Appendix A supports this model but the results may not be conclusive because of its simplicity and it contains large uncertainties in the estimation of the maximum extents of swelling. Precise interpretation would require knowledge of the spatial composition of the film, along the lines of that described by Hinsberg et al. [16] or using confocal microscopy. For this case, the observed behaviour is counter-intuitive. After all, if the PPX layer is swollen, then one might expect it to dissolve and the PPM layer thereby be washed away—but it does not. Further investigation will be required to elucidate this behaviour.

4. Conclusions

This paper demonstrates the usefulness of fluid dynamic gauging in studying and quantifying the mechanisms arising in solvent cleaning of emulsion polymerization reactors. The thickness of the fouling layers can be monitored in situ and in real time over a useful range of experimental parameters. Further data such as initial swelling rates and induction periods could be obtained using customized apparatus, while the strength of the foulant layers could also be probed using FDG in its force mode. The findings, in particular those from cleaning of composite layers, provide useful guidance for solvent selection, reactor operation and cleaning scheduling.

Cleaning experiments on PX, PA and the pilot plant samples showed four types of outcomes. Firstly, no removal was observed in sodium hydroxide and metasilicate. PX and PA swelled only after an induction period. Stamatialis et al. [13] classified this as non-solvent behaviour. Secondly, PX and PA swelled immediately on contact with MEK, followed by complete dissolution. This behaviour was also observed for PX in TPU but at a slower rate. The third outcome is the self-detachment of PA in TPU after substantial swelling. Lastly, MEK and TPU partially dissolved the pilot plant sample (mainly PMMA), leaving an undissolved residue. All the results showed that MEK generally worked fastest among the solvents considered.

Experiments on composite films suggested that the removal behaviour of such films could be predicted from the rates of swelling and dissolution of their individual layers, and

thereby offer guidance for scheduling of batch reaction and cleaning.

The pilot plant PX films (PPX) showed that the rates of swelling and dissolution compared closely to laboratory PX films. PPM left a residue which could not be removed by chemical action alone, and this tended to inhibit the removal of swollen or dissolved material underneath it.

Acknowledgements

Support for this work from NeoResins is gratefully acknowledged, as is funding for JYMC from the Cambridge Overseas Trust. Contributions from Dennis Keight, Alan Gould, Rob van den Born, Rob Arnoldus and Roeland Krap are all gratefully acknowledged, as is the assistance of the NeoResins pilot plant team.

Appendix A. Estimations of pilot plant behaviour

A.1. PPX on PPM

Consider the case for [PPX on PPM] in TPU at 90 °C, in Fig. 10(a). It is reasonable to assume that PPM starts to swell only after completion of the swelling of PPX (this observation is consistent with Case II diffusion, i.e. the presence of an advancing front) and that both layers swelled completely to reach equilibrium thickness. The residual layer in Fig. 10(a) is expected to be only PPM since the PPX layer on top would have dissolved completely after ~44 min. This postulate can be tested by a simple analysis as follows.

For the swollen composite film, let x be the volume fraction of swollen PPX so that $1-x$ is the fraction of PPM. Therefore,

$$\begin{aligned}&\varepsilon_{\max,\text{composite}} = x\varepsilon_{\max,\text{PPX}} + (1-x)\varepsilon_{\max,\text{PPM}}\\ &0.33 = x\cdot 0.25 + (1-x)\cdot 0.42\end{aligned} \quad \text{(A.1)}$$

Solving Eq. (A.1) gives $x = 0.56$ and $1-x = 0.44$. The maximum thickness of swollen PPM in the composite film is therefore

$$\text{swollen PPM} = (1-x)\text{swollen composite film} \quad \text{(A.2)}$$

giving $\delta_{\max,\text{PPM}} = 0.44 \times 0.27 = 0.12$ mm. For PPM alone in TPU (Fig. 9(b)), the depth of the residue, $\delta_{\text{residue,PPM}}$, and the maximum thickness, $\delta_{\max,\text{PPM}}$, are, respectively, 0.05 and 0.14 mm. The ratio of these is,

$$\frac{\delta_{\text{residue,PPM}}}{\delta_{\max,\text{PPM}}} \sim \frac{0.05}{0.14} = 0.35 \quad \text{(A.3)}$$

The depth of the residue, $\delta_{\text{residue,PPM}}$, in the composite film is predicted using the ratio calculated from Eq. (A.3),

$$\delta_{\text{residue,PPM}} = \delta_{\max,\text{PPM}} \times 0.35$$
$$\delta_{\text{residue,PPM}} = 0.12 \times 0.35 = 0.04\,\text{mm}$$

The predicted value of $\delta_{\text{residue,PPM}} \sim 0.04$ mm is the same as that observed for [PPX on PPM] in TPU at 90 °C in Fig. 10(a). This is consistent with the assumptions that both layers swelled completely and that the residue was composed only of swollen PPM.

A.2. PPM on PPX

The same analysis, with the assumption that both layers swelled completely, is applied to the case for PPM on PPX in Fig. 10(b). Here, the depth of the residue is significantly greater than that for PPX on PPM. The postulation is that the residue is composed of both PPM and PPX because the undissolved PPM layer prevents PPX from dissolving. Solving Eq. (A.1) in this case yields $x = 0.60$ and $1-x = 0.40$. The maximum thickness of swollen PPM in the composite film is (Eq. (A.2)), $\delta_{\max,\text{PPM}} = 0.40 \times 0.19 = 0.08$ mm. The depth of the residue composed of swollen PPM, $\delta_{\text{residue,PPM}}$, in the composite film is predicted using the ratio calculated from Eq. (A.3),

$$\delta_{\text{residue,PPM}} = \delta_{\max,\text{PPM}} \times 0.35 = 0.08 \times 0.35 = 0.03\,\text{mm}$$

This value is significantly less than the observed thickness for PPM/PPX, i.e. 0.13 mm. It is then clear that the residue also consists of PPX either fully or partially swelled.

The predicted depth of the residue composed of PPX, $\delta_{\text{residue,PPX}}$, in the composite film is,

$$\delta_{\text{residue,PPX}} = \delta_{\text{residue,composite}} - \delta_{\text{residue,PPM}}$$
$$\Rightarrow \delta_{\text{residue,PPX}} = 0.13 - 0.03 = 0.10\,\text{mm}$$

The maximum thickness attainable assuming PPX swelled completely in the composite film is

$$\delta_{\max,\text{PPX}} = x \times \delta_{\max,\text{composite}} = 0.60 \times 0.19 = 0.11\,\text{mm} \quad \text{(A.4)}$$

This prediction for $\delta_{\text{residue,PPX}} \sim 0.10$ mm is marginally less than that calculated when PPX was assumed to swell completely, i.e. 0.11 mm. This inconsistency might suggest that the top PPM prevented the lower PPX layer from swelling fully, thereby preventing it from dissolving. The discrepancy in $\delta_{\text{residue,PPX}}$, however, is marginal and may be due to the uncertainties in the estimation of $\varepsilon_{\max}$ when calculating the fractions of PPX and PPM in the composite film. A conclusive interpretation would require knowledge of the initial compositions of the films. However, these calculations do indicate that the PPX is not unswollen. It follows that TPU must have penetrated the PPM layer, so that the PPM residue itself is presumably fully swollen.

Note that this analysis is not applied to pilot plant samples cleaned in MEK because the processes in MEK were rapid and the sharp peaks in the removal profiles suggest that equilibrium swelling was not reached.

References

[1] M.S. El-Aasser, E.D. Sudol, Features of emulsion polymerization, in: P.A. Lovell, M.S. El-Aasser (Eds.), Emulsion Polymerization and Emulsion Polymers, John Wiley & Sons Ltd., London, UK, 1997.
[2] J.W. Vanderhoff, The formation of coagulum in emulsion polymerization, in: D.R. Basset, A. Hamielec (Eds.), Emulsion Polymers and Emulsion Polymerization, American Chemical Society, NY, USA, 1981, p. 165.
[3] A. Perka, C.S. Grant, M.R. Overcash, Waste minimization in batch vessel cleaning, Chem. Eng. Commun. 119 (1993) 167.
[4] B. Hunek, E.L. Cussler, Mechanisms of photoresist dissolution, AIChE J. 48 (4) (2002) 661.

[5] J.A. Kabin, A.E. Saéz, C.S. Grant, R.G. Carbonnell, Removal of organic films from rotating disks using aqueous solutions of non-ionic surfactants: film morphology and cleaning mechanisms, Ind. Eng. Chem. Res. 35 (12) (1996) 4494.
[6] J.A. Kabin, S.T. Withers, C.S. Grant, R.G. Carbonnell, A.E. Saéz, Removal of solid organic films from rotating disks using emulsion cleaners, J. Colloid Interface Sci. 228 (2) (2000) 344.
[7] W. Liu, G.K. Christian, Z. Zhang, P.J. Fryer, Development and use of a micromanipulation technique for measuring the force required to disrupt and remove fouling deposits, Food Bioprod. Proc. 80 (C4) (2002) 286.
[8] K.R. Morison, R.J. Thorpe, Liquid distribution from cleaning-in-place sprayballs, Food Bioprod. Proc. 80 (C4) (2002) 270.
[9] T.R. Tuladhar, W.R. Paterson, N. Macleod, D.I. Wilson, Development of a novel non-contact proximity gauge for thickness measurement of soft deposits and its application in fouling studies, Can. J. Chem. Eng. 78 (2000) 935.
[10] J.Y.M. Chew, S.S.S. Cardoso, W.R. Paterson, D.I. Wilson, CFD studies of dynamic gauging, Chem. Eng. Sci. 59 (2004) 3381.
[11] N. Macleod, R.B. Todd, The experimental determination of wall-fluid mass transfer coefficient using plasticized polymer surface coatings, Int. J. Heat Mass Transfer 16 (1973) 485.
[12] J.Y.M. Chew, Development of fluid dynamic gauging for cleaning studies, Ph.D. Dissertation, University of Cambridge, 2004.
[13] D.F. Stamatialis, M. Sanopoulou, I. Raptis, Swelling and dissolution behavior of poly(methyl methacrylate) films in methylethylketone/methyl alcohol mixtures studies by optical techniques, J. Appl. Polym. Sci. 83 (2002) 2823.
[14] R.O. Ebewele, Polymer Science and Technology, CRC Press, FL, USA, 2000.
[15] I. Devotta, V.D. Ambeskar, A.B. Mandhare, R.A. Mashelkar, The life time of a dissolving polymeric particle, Chem. Eng. Sci. 49 (5) (1994) 645.
[16] W. Hinsberg, F.A. Houle, H. Ito, Characterization of reactive dissolution and swelling of polymer films using quartz crystal microbalance and visible and infrared reflectance spectroscopy, Macromolecules 38 (2005) 1882.
[17] J.Y.M. Chew, W.R. Paterson, D.I. Wilson, Dynamic gauging for measuring the strength of soft deposits, J. Food Eng. 65 (2) (2004) 175.
[18] J.Y.M. Chew, S.J. Tonneijk, W.R. Paterson, D.I. Wilson, Mechanisms in the solvent cleaning of emulsion polymerization reactor surfaces, Ind. Eng. Chem. Eng. Res. 44 (13) (2005) 4605.